

Neural Probabilistic Shaping: Joint Distribution Learning for Optical Fiber Communications

Mohammad Taha Askari⁽¹⁾, Lutz Lampe⁽¹⁾, Amirhossein Ghazisaeidi⁽²⁾

⁽¹⁾ Department of Electrical and Computer Engineering, University of British Columbia, Vancouver, BC V6T 1Z4, Canada, mohammadtaha@ece.ubc.ca

⁽²⁾ Nokia Bell Labs, 12 rue Jean Bart, 91300 Massy, France

Abstract We present an autoregressive end-to-end learning approach for probabilistic shaping on nonlinear fiber channels. Our proposed scheme learns the joint symbol distribution and provides a 0.3-bits/2D achievable information rate gain over an optimized marginal distribution for dual-polarized 64-QAM transmission over a single-span 205 km link. ©2025 The Author(s)

Introduction

Probabilistic shaping (PS) has been widely adopted in communication systems to approach channel capacity by optimizing the symbol distribution^[1]. While PS is known to provide linear shaping gains over the additive white Gaussian noise (AWGN) channel, it can also yield additional gains in optical fiber systems when the distribution is carefully tailored to account for channel nonlinearities and memory^[2]. The work in^[3] showed that shaping over symbol sequences under an energy constraint can provide nonlinear shaping gains, with the optimal block length closely tied to channel memory. Furthermore, finite blocklength shaping methods such as enumerative sphere shaping (ESS)^[4] have been shown to mitigate nonlinear interference noise (NLIN)^[5]. Subsequent studies revealed that differences in temporal symbol structures, i.e., joint distributions, can significantly affect NLIN characteristics^{[2],[6]}.

Sequence selection is an indirect method for optimizing joint symbol distributions using rejection sampling^[7]. This approach generates multiple symbol sequences and selects those that minimize NLIN using a nonlinearity-aware metric^{[2],[8]}. Although effective in shaping joint distributions, the method does not ensure optimality because the quality of candidate sequences is uncontrolled, and the selection metrics may not fully capture channel impairments or digital signal processing (DSP) effects. Consequently, numerous candidate sequences are required to achieve meaningful performance gains, increasing computational complexity and incurring additional rate loss^[9].

Autoencoder (AE) neural networks can directly optimize PS by modeling the transmitter, channel, and receiver as a single differentiable system for end-to-end (E2E) optimization. In^[10], a symbol-wise AE generates logits for a marginal distribution and uses the Gumbel-softmax trick^[11] for differentiable sampling and the cross-entropy loss to maximize mutual information over the AWGN channel.

Later,^[12] introduced a bit-wise AE that jointly optimizes symbol distribution, bit labeling, and demapping to maximize bit-metric information using log-likelihood ratios (LLRs). E2E learning has also been applied to both coherent and non-coherent optical fiber systems^{[13]–[15]}. However, most existing work focuses on the marginal symbol distribution, which is suboptimal in channels with significant nonlinearity and memory. Only a few studies have attempted to incorporate memory effects: one using a learned pre-distortion filter while still relying on marginal-distribution shaping^[16], and another explores joint-distribution learning over two-symbol blocks in a four-dimensional constellation, though without scalability to longer sequences^[17].

This paper introduces a new E2E learning framework that directly optimizes the joint distribution of symbol sequences for nonlinear fiber channels. Its core is a recurrent neural network (RNN) to generate conditional symbol distributions using Gumbel-softmax sampling for gradient-based training. We refer to this architecture as neural PS (NPS). The framework supports any differentiable channel model and DSP module and can be implemented in a distribution matcher without the rate loss inherent to sequence selection. Numerical results show that joint-distribution learning with NPS improves achievable information rate (AIR) and mitigates NLIN more effectively than marginal-distribution shaping, finite-blocklength shaping, or sequence selection.

Problem Statement

To enable sequence-level PS, we aim to learn a joint distribution over transmitted symbols that maximizes the AIR under bit-metric decoding (BMD). Let $\mathbf{x} = (x_1, \dots, x_L)$ and $\mathbf{y} = (y_1, \dots, y_L)$ denote the transmitted and received sequences of length L , respectively. Each transmitted symbol x_t is drawn from an M -ary constellation set $\mathcal{C} = \{c_1, \dots, c_M\}$ and is associated with a binary label $\mathbf{b}_t = (b_t^{(1)}, \dots, b_t^{(m)})$, where $m = \log_2(M)$.

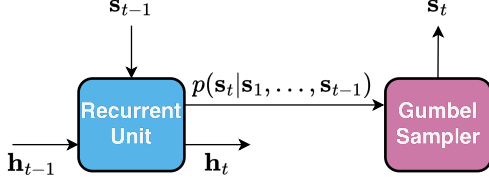


Fig. 1: NPS encoder block diagram at time step t . \mathbf{h}_t is the recurrent context vector, and $p(s_t | s_1, \dots, s_{t-1})$ is the predicted conditional distribution. The one-hot vector s_t , representing the transmitted symbol x_t , is sampled from this distribution using the Gumbel-softmax trick.

The learning objective is to optimize the joint distribution $p(\mathbf{x})$ to maximize the AIR, which for BMD can be written as^[12]

$$\arg \max_{p(\mathbf{x})} \sum_{t=1}^L \left[\underbrace{H(\mathbf{b}_t) - \sum_{i=1}^m H(b_t^{(i)} | \mathbf{y})}_{R_t} \right] \quad (1)$$

$$\text{subject to } \sum_{\mathbf{x}} p(\mathbf{x}) \|\mathbf{x}\|^2 = 1, \quad (2)$$

where $H(\cdot)$ denotes entropy, R_t is the AIR contribution from the t -th symbol, and the constraint enforces unit average transmit power. Since directly optimizing the M^L -dimensional joint distribution is intractable, we seek a structured and trainable parameterization. In the next sections, we present the NPS architecture designed to efficiently model this distribution while enabling E2E optimization through gradient-based learning.

Neural Probabilistic Shaping Encoder

The core idea is to use an encoder that parameterizes the factorized joint distribution $p(\mathbf{x})$ using an autoregressive model. At each time step t , the encoder generates the logits for the conditional distribution $p(x_t | x_1, \dots, x_{t-1})$, based on the previous symbol x_{t-1} and a recurrent context vector \mathbf{h}_{t-1} . A sample is drawn from this distribution using the Gumbel-softmax trick, yielding a soft one-hot vector that is passed through a straight-through estimator^[18] and mapped to a constellation symbol x_t , following the sampling approach in^[10]. Figure 1 illustrates the recurrent operation at time step t for the NPS encoder architecture. This step is repeated L times to sample the sequence \mathbf{x} from the joint distribution. While the encoder generates the conditional distributions, we apply the scaling

$$\frac{1}{L} \sum_{t=1}^L \sum_{i=1}^M p(x_t = c_i) |c_i|^2 = 1 \quad (3)$$

as a proxy to the unit power constraint in (2), where the marginal symbol probabilities $p(x_t)$ are obtained from Monte Carlo estimation.

Gumbel-softmax sampling in NPS preserves differentiability during joint-distribution learning.

For practical deployment, we propose replacing it with arithmetic distribution matching^[19], which maps information bits to output symbols based on the learned conditional distributions, similar to context-based source coding with adaptive arithmetic coding^[20].

Channel Model

To account for channel memory inherent in optical fiber transmission, multiple symbol sequences \mathbf{x} are generated using the encoder and concatenated before transmission. The combined sequence is passed through a channel modeled by the additive-multiplicative formulation of the first-order perturbative model as^[2]

$$y_t = x_t \exp \left(j\gamma \sum_n (|x_{t-n}|^2 - 1) c_n \right) + \Delta x_t + n_t, \quad (4)$$

where γ is the fiber nonlinearity coefficient, c_n denotes the perturbation coefficient^[21] associated with the nonlinear phase rotation, Δx_t represents the additive NLIN arising from signal-signal interactions, and n_t is the lumped amplified spontaneous emission (ASE) noise at time t . We use this perturbative channel model for its simplicity, which speeds up training. More accurate models can also be applied.

Decoder and Loss Function

At the receiver, we discard symbols from the beginning and end of the transmission window to fully capture channel memory effects. The remaining samples are then processed by a mismatched Gaussian demapper, where the output LLRs are used to compute the binary cross entropy (BCE) loss summed across the L received symbols as

$$\mathcal{L} = \sum_{t=1}^L \sum_{i=1}^m \mathbb{E} \left[-\log \tilde{p}(b_t^{(i)} | y_t) \right], \quad (5)$$

where \mathbb{E} indicates statistical expectation and $\tilde{p}(b_t^{(i)} | y_t)$ denotes the mismatched Gaussian posterior. The loss (5) can be decomposed as

$$\mathcal{L} = \sum_{t=1}^L \left(H(\mathbf{b}_t) - R_t + \sum_{i=1}^m \mathbb{E} \left[D_{\text{KL}}(p(b_t^{(i)} | \mathbf{y}) \| \tilde{p}(b_t^{(i)} | y_t)) \right] \right), \quad (6)$$

where D_{KL} is the Kullback–Leibler (KL) divergence. For training, we adopt the adjusted loss $\hat{\mathcal{L}} = \mathcal{L} - \sum_{t=1}^L H(\mathbf{b}_t)$, which encourages maximization of AIR, consistent with^{[10],[12]}. Although the KL divergence between the true posterior and the mismatched Gaussian approximation in (6) could be minimized using a learned demapper, we intentionally fix the demapper in this work to isolate the effects of transmitter-side distribution learning from receiver-side compensation.

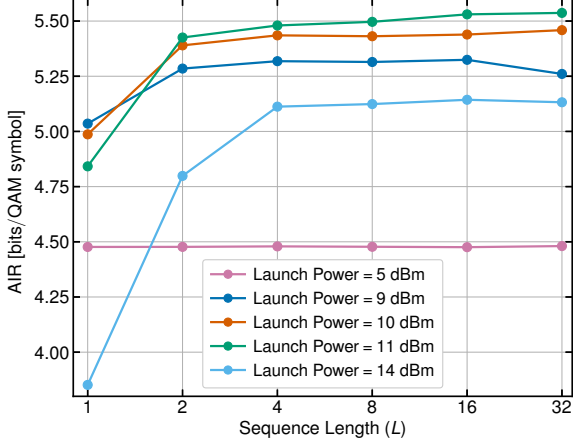


Fig. 2: AIR vs. sequence length for different launch powers during training and the perturbative channel model.

Numerical Results

We adopt the simulation setup from [6], [22], considering a dual-polarization 64-QAM wavelength division multiplexing (WDM) system with 5 channels, a baud rate of 50 GBaud, and 55 GHz channel spacing. Symbols are pulse shaped using a root raised-cosine filter with a 0.1 roll-off factor. The fiber link is simulated using the split-step Fourier method (SSFM) and consists of a single span of 205 km standard single-mode fiber with attenuation coefficient of 0.2 dB/km, chromatic dispersion of 17 ps/nm/km, and nonlinearity coefficient of $1.3 \text{ W}^{-1}\text{km}^{-1}$. At the receiver, an Erbium-doped fiber amplifier (EDFA) with noise figure 5 dB is used. Chromatic dispersion is electronically compensated, and a linear pilot-aided carrier phase recovery with a pilot rate of 2.5% is applied [23]. The performance metrics for the central channel are reported.

NPS encoder training: We train the NPS encoder with output sequence length L for each launch power using backpropagation through a single-channel, single-polarization perturbation model as described in (4). The recurrent unit comprises a single-layer long short-term memory (LSTM) network [24] with a hidden size of 256, and a linear layer that maps the hidden states to the constellation space of size $M = 64$. Fig. 2 shows the AIR as a function of sequence length L for models trained at different launch powers under this perturbative model. In the low power regime, joint-distribution learning (i.e., $L > 1$) offers little benefit because the channel behaves approximately linearly. However, at higher launch powers, learning the joint distribution significantly improves AIR compared to marginal-distribution shaping (i.e., $L = 1$). Moreover, the optimal launch power shifts from 9 dBm at $L = 1$ to 11 dBm at $L = 32$, indicating that joint-distribution learning enhances NLIN tolerance.

SSFM simulations: Next, we evaluate the performance of neural encoders trained with $L = 1$ and $L = 32$ at their respective optimal launch powers

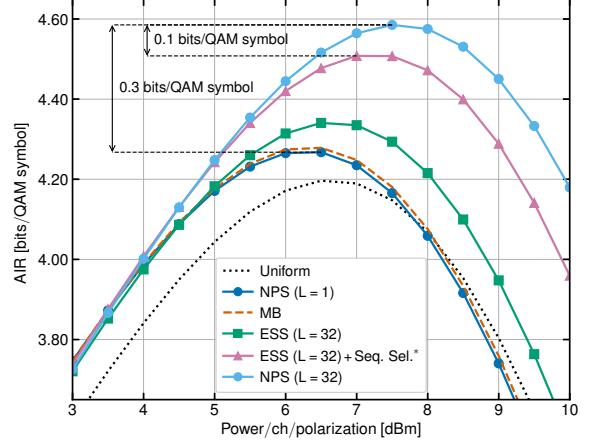


Fig. 3: AIR vs. launch power for different sequence lengths. A dual-polarization WDM channel is simulated using SSFM.

by generating sequences and testing them across a range of launch powers. Figure 3 shows the AIR versus launch power for the dual-polarization WDM channel simulated using SSFM. The AIR for uniform distribution is included as a baseline. We compare against transmission with a Maxwell-Boltzmann (MB) distribution matched to the entropy of the NPS encoder with $L = 1$, ESS with blocklength 32, and ESS with sequence selection with 64 candidate sequences using the additive-multiplicative metric from [25]. The ESS rate loss due to finite-length shaping is compensated to have a fair comparison. Furthermore, we did not deduct the sequence-selection rate loss to highlight the advantage of directly learning the joint distribution by NPS. Thus, we show an upper performance bound for sequence selection.

NPS with $L = 1$ matches the performance of the MB distribution, outperforming the uniform case for most launch powers. ESS and ESS with sequence selection provide further significant improvements. However, NPS with $L = 32$ outperforms all other methods including the upper bound for ESS with sequence selection. At optimum launch power, the AIR gains are 0.3 bits/2D over optimized marginal PS and 0.1 bits/2D over the sequence selection bound. Additionally, the optimal launch power is largest for NPS with $L = 32$, demonstrating its improved robustness to NLIN.

Conclusions

We proposed neural probabilistic shaping for non-linear optical fiber channels. NPS employs an RNN with Gumbel-softmax sampling to directly model the joint symbol distribution, capturing temporal dependencies for improved performance over marginal-distribution shaping. Unlike sequence selection, it avoids additional rate loss and reduces complexity. SSFM simulations demonstrate substantial AIR gains and enhanced NLIN robustness, underscoring the effectiveness of neural sequence modeling for PS in optical systems.

Acknowledgements

This work was supported by Nokia Bell Labs, France; the Mitacs Accelerate International program; the Institute for Computing, Information and Cognitive Systems (ICICS) at UBC; and the Digital Research Alliance of Canada (www.alliancecan.ca).

References

- [1] G. Böcherer, F. Steiner, and P. Schulte, "Bandwidth efficient and rate-matched low-density parity-check coded modulation", *IEEE Transactions on Communications*, vol. 63, no. 12, pp. 4651–4665, 2015. DOI: 10.1109/TCOMM.2015.2494016.
- [2] M. T. Askari and L. Lampe, "Probabilistic shaping for nonlinearity tolerance", *Journal of Lightwave Technology*, vol. 43, no. 4, pp. 1565–1580, 2025. DOI: 10.1109/JLT.2024.3521642.
- [3] R. Dar, M. Feder, A. Mecozzi, and M. Shtaif, "On shaping gain in the nonlinear fiber-optic channel", in *2014 IEEE International Symposium on Information Theory*, 2014, pp. 2794–2798. DOI: 10.1109/ISIT.2014.6875343.
- [4] A. Amari, S. Goossens, Y. C. Gültekin, *et al.*, "Introducing enumerative sphere shaping for optical communication systems with short blocklengths", *Journal of Lightwave Technology*, vol. 37, no. 23, pp. 5926–5936, 2019. DOI: 10.1109/JLT.2019.2943938.
- [5] T. Fehenberger, D. S. Millar, T. Koike-Akino, K. Kojima, K. Parsons, and H. Griesser, "Analysis of nonlinear fiber interactions for finite-length constant-composition sequences", *Journal of Lightwave Technology*, vol. 38, no. 2, pp. 457–465, 2020. DOI: 10.1109/JLT.2019.2937926.
- [6] M. T. Askari, L. Lampe, and J. Mitra, "Probabilistic amplitude shaping and nonlinearity tolerance: Analysis and sequence selection method", *Journal of Lightwave Technology*, vol. 41, no. 17, pp. 5503–5517, 2023. DOI: 10.1109/JLT.2023.3264032.
- [7] M. Secondini, S. Civeili, E. Forestieri, and L. Z. Khan, "New lower bounds on the capacity of optical fiber channels via optimized shaping and detection", *Journal of Lightwave Technology*, vol. 40, no. 10, pp. 3197–3209, 2022. DOI: 10.1109/JLT.2022.3148322.
- [8] S. Civeili, E. Forestieri, and M. Secondini, "Sequence-selection-based constellation shaping for nonlinear channels", *Journal of Lightwave Technology*, vol. 42, no. 3, pp. 1031–1043, 2024. DOI: 10.1109/JLT.2023.3332487.
- [9] S. Civeili and M. Secondini, "Cost-gain analysis of sequence selection for nonlinearity mitigation", *arXiv preprint arXiv:2411.02004*, 2024.
- [10] M. Stark, F. Ait Aoudia, and J. Hoydis, "Joint learning of geometric and probabilistic constellation shaping", in *IEEE Global Communications Conference (GlobeCom)*, 2019, pp. 1–6. DOI: 10.1109/GCOWkshps45667.2019.9024567.
- [11] E. Jang, S. Gu, and B. Poole, "Categorical reparameterization with gumbel-softmax", in *International Conference on Learning Representations (ICLR)*, 2017. [Online]. Available: <https://openreview.net/forum?id=rkE3y85ee>.
- [12] F. A. Aoudia and J. Hoydis, "Joint learning of probabilistic and geometric shaping for coded modulation systems", in *IEEE Global Communications Conference (GlobeCom)*, 2020, pp. 1–6. DOI: 10.1109/GLOBECOM42002.2020.9348032.
- [13] B. Karanov, M. Chagnon, F. Thouin, *et al.*, "End-to-end deep learning of optical fiber communications", *Journal of Lightwave Technology*, vol. 36, no. 20, pp. 4843–4855, 2018. DOI: 10.1109/JLT.2018.2865109.
- [14] A. Rode, B. Geiger, S. Chimmalggi, and L. Schmalen, "End-to-end optimization of constellation shaping for wiener phase noise channels with a differentiable blind phase search", *Journal of Lightwave Technology*, vol. 41, no. 12, pp. 3849–3859, 2023. DOI: 10.1109/JLT.2023.3265308.
- [15] V. Neskorniyuk, A. Carnio, D. Marsella, S. K. Turitsyn, J. E. Prilepsky, and V. Aref, "Model-based deep learning of joint probabilistic and geometric shaping for optical communication", in *Conference on Lasers and Electro-Optics (CLEO)*, 2022, pp. 1–2.
- [16] V. Neskorniyuk, A. Carnio, D. Marsella, S. K. Turitsyn, J. E. Prilepsky, and V. Aref, "Memory-aware end-to-end learning of channel distortions in optical coherent communications", *Optics Express*, vol. 31, no. 1, pp. 1–20, 2022. DOI: 10.1364/oe.470154.
- [17] X. Liu, I. Darwazeh, N. Zein, and E. Sasaki, "Probabilistic shaping for multidimensional signals with autoencoder-based end-to-end learning", in *IEEE Wireless Communications and Networking Conference (WCNC)*, 2022, pp. 2619–2624. DOI: 10.1109/WCNC51071.2022.9771910.
- [18] Y. Bengio, N. Léonard, and A. Courville, "Estimating or propagating gradients through stochastic neurons for conditional computation", *arXiv preprint arXiv:1308.3432*, 2013.
- [19] S. Baur and G. Böcherer, "Arithmetic distribution matching", in *International ITG Conference on Systems, Communications and Coding (SGC)*, 2015, pp. 1–6.
- [20] D. Marpe, H. Schwarz, and T. Wiegand, "Context-based adaptive binary arithmetic coding in the H.264/AVC video compression standard", *IEEE Transactions on Circuits and Systems for Video Technology*, vol. 13, no. 7, pp. 620–636, 2003. DOI: 10.1109/TCSVT.2003.815173.
- [21] A. Ghazisaeidi and R.-J. Essiambre, "Calculation of coefficients of perturbative nonlinear pre-compensation for nyquist pulses", in *The European Conference on Optical Communication (ECOC)*, 2014, pp. 1–3. DOI: 10.1109/ECOC.2014.6964065.
- [22] Y. C. Gültekin, A. Alvarado, O. Vassilieva, *et al.*, "Kurtosis-limited sphere shaping for nonlinear interference noise reduction in optical channels", *Journal of Lightwave Technology*, vol. 40, no. 1, pp. 101–112, 2022. DOI: 10.1109/JLT.2021.3120915.
- [23] P. Nesaastegaran and A. H. Banihashemi, "Log-likelihood ratio calculation for pilot symbol assisted coded modulation schemes with residual phase noise", *IEEE Transactions on Communications*, vol. 67, no. 5, pp. 3782–3790, 2019. DOI: 10.1109/TCOMM.2019.2896190.
- [24] S. Hochreiter and J. Schmidhuber, "Long short-term memory", *Neural Computation*, vol. 9, no. 8, pp. 1735–1780, 1997. DOI: 10.1162/neco.1997.9.8.1735.
- [25] M. T. Askari and L. Lampe, "Perturbation-based sequence selection for probabilistic amplitude shaping", in *European Conference on Optical Communication (ECOC)*, 2024, pp. 846–849.